Atomization and Sprays, 26 (10): 1031–1050 (2016)

ATOMIZATION OF MOLTEN MATERIALS FOR PARTICLE COATING: PREDICTION OF MEAN DROPLET SIZE FOR TWO-FLUID NOZZLES

Consuelo Pacheco,[1,*] Juliana Piña,[2] & Khashayar Saleh[1]

[1] *Temporarily at Laboratoire TIMR/EA 4297, Département Génie des Procédés, Université de Technologie de Compiègne, 60205 Compiègne CEDEX, France*

[2] *Planta Piloto de Ingeniería Química, Universidad Nacional del Sur, 8000 Bahía Blanca, Argentina*

[*] Address all correspondence to: Consuelo Pacheco,
E-mail: cpacheco@plapiqui.edu.ar

Original Manuscript Submitted: 01/06/2015; Final Draft Received: 04/21/2015

Coating is the process of covering solid particles' surfaces with a homogeneous layer of a coating agent comprising one or multiple components. For processes carried out in fluidized beds, coating is achieved by spraying the coating agent on the particles in suspension. The aim of the present work was to study the atomization of molten materials prior to their application to powder coating in fluidized beds. Several external mixing binary nozzles were used for the atomization of a stearic–palmitic acid mixture and different polyethylene glycol grades (1000, 1500, 2050, 4000, and 6000) at different temperatures (60°C, 70°C, 80°C, and 90°C). The droplet size distributions, from which experimental mean droplet sizes were calculated, were measured by the laser diffraction technique. Subsequently, mean droplet sizes were satisfactorily modeled using different correlations reported in the literature. For a given nozzle, it was found that some fitting parameters were constant for all the polyethylene glycol grades, whereas others showed a dependency with the material viscosity. This latter was the property with the highest variability over the experimental domain. The fitted models did not provide a good prediction of the experimental data corresponding to different nozzle configurations or molten materials; therefore, new fittings were performed. This fact highlights the difficulty in obtaining models at least applicable to the atomization of molten materials.

KEY WORDS: *atomization, hot-melt coating agent, mean droplet size*

1. INTRODUCTION

Powder coating and encapsulation have gained great attention in recent years. These techniques are generally performed to achieve one or several of the following objectives:

 © 2016 by Begell House, Inc.

to protect powders from ambient factors; to delay and/or control the release of active agents; to confer desired interfacial properties or desired particle size; to improve product appearance, taste, or odor; to conserve nutrients contained in food products; and to functionalize powders (catalysts, enzyme-coated detergents, etc.) (Saleh and Guigon, 2007a).

The coating process involves the deposition of a homogeneous layer of a coating agent comprising one or multiple components onto solid particles (Saleh and Guigon, 2007b). It can be performed with different equipment, fluidized beds being the most widespread in the industry (Saleh and Guigon, 2007a). In these units, coating is achieved by atomizing the coating agent over the suspended particles. The agent can be introduced in several manners: dispersed or dissolved in an easily evaporable solvent (wet coating), molten (hot-melt coating), or in powder form (dry powder coating) (Saleh and Guigon, 2007b). Nowadays, wet coating is the most widely applied coating process. However, hot-melt coating possesses various advantages related to the absence of solvent. For instance, it has no requirement for solvent evaporation and drying, implying shorter processing time and reduced energy consumption; it offers cleaner and safer operations with respect to those processes based on organic solvents; it is a more cost-effective operation owing to the elimination of the expensive organic solvent disposal stage; and, in many cases, it leads to higher product quality because of the absence of residual solvent in the product and no solvent exposure during processing (Bose and Bogner, 2007; Borini et al., 2009; Kulah and Kaya, 2011).

Atomization is the process of converting a bulk liquid into a multiplicity of small drops (Kashani, 2010), which is accomplished by applying a high relative velocity between the liquid and surrounding gas phase so that the disruptive aerodynamic force exceeds the consolidating surface tension force (Lefebvre, 1989). Depending on how this relative velocity is achieved, nozzles can be divided into two main categories: (1) pressure or single-fluid nozzles, for which the pressurized liquid is the only stream fed to the device, and (2) pneumatic or two-fluid nozzles, in which two streams are fed, a liquid and a gas—in most cases, air (Lefebvre, 1989). Droplet formation arises from different phenomena in each case. In the first one, the liquid energy pressure is transformed into kinetic energy when it accelerates through the nozzle and the relative velocity between the liquid and the quiescent air generates instabilities within the liquid that finally lead to the disintegration of the liquid jet into droplets (Walzel, 2012). In two-fluid nozzles, the pressure of the compressed air is used to disperse the liquid into small droplets thanks to the shear forces, which are exerted by the air of atomization on the liquid surface (Jiménez, 2007). These nozzles can be further classified according to the site where both fluids come into contact: (2a) the internal mixing nozzles, for which contact is accomplished inside the device, and (2b) the external mixing ones, featuring the contact at the exit of the nozzle (Hede et al., 2008). External mixing nozzles enable greater control of atomization by independent control of both liquid and air streams, and for that reason, external mixing nozzles are typically preferred for fluid-bed

processes. Furthermore, this configuration reduces the risk of nozzle clogging (Hede et al., 2008).

Atomization conditions are one of the most critical factors in coating processes. Experience indicates that knowledge and control *a priori* of droplet size distribution and mean droplet diameter are vital to the processes' success (Hede et al., 2008). Even so, droplet size data from scientific studies of two-fluid atomization nozzles are scarce, partly inconsistent (Hede et al., 2008), and mostly obtained from the atomization of solutions.

Droplet size distributions are often characterized by the Sauter mean diameter (d_{32}, defined as the diameter of a droplet with an equal surface to volume ratio as the population it characterizes). The Sauter mean diameter depends on the physicochemical properties of fluids, nozzle design, and operating conditions (Semião et al., 1996). The contribution of the liquid physicochemical properties has been attributed to surface tension, viscosity, and density effects. It is widely accepted that an increase in liquid surface tension, viscosity, and/or density will lead to a greater droplet size (Rizkalla and Lefebvre, 1975; Lefebvre, 1980; Hede et al., 2008; Ejim et al., 2010), although this last property appears to have little effect on the mean drop size (Lefebvre, 1989). Operating conditions also have an important effect; the droplet size increases when the liquid flow is increased or the air pressure is decreased (Hede et al., 2008), where the influence of this last operating condition is notably greater than that of the first one (Mandato et al., 2012). The higher the liquid viscosity is, the lower is the sensitivity of the drop size to the air density and velocity and to the air to liquid mass flow ratio (ALR) (Lefebvre, 1980).

Mean droplet sizes, as the Sauter mean diameter, are centralization parameters essential for the characterization of droplet size distributions. Nonetheless, the latter are not fully described until a parameter that accounts for their dispersion or uniformity is given. The relative span factor (RSF) is a dimensionless dispersion parameter commonly used in atomization studies (Genbao et al., 2012; Nuyttens et al., 2007).

The aim of the present work is to perform a study of the atomization of molten materials prior to their use for powder coating in fluidized beds. By means of different two-fluid external nozzles with different spray patterns, several grades of polyethylene glycol (PEG) (1000, 1500, 2050, 4000, and 6000) and a mixture of stearic and palmitic acids was atomized at different temperatures (60ºC, 70ºC, 80ºC, and 90ºC). PEG is a hydrophilic polymer, whereas the mixture of fatty acids possesses a hydrophobic character. Both materials are largely used as coating agents in the pharmaceutical industry, although for different applications because of their different water affinities. Different PEG grades and temperatures were selected to vary the physicochemical properties. Various operating conditions were applied to analyze their influence on the mean droplet size. Mean drop size and RSF were calculated from the droplet size distributions, which were determined by the laser diffraction technique. By using correlations reported in the open literature and parameter fitting, the experimental mean droplet sizes were satisfactorily modeled.

2. MATERIAL AND METHODS

2.1 Material

2.1.1 Atomizing Systems

Table 1 presents the different atomizing systems employed, which are characterized by diverse dimensions and spray patterns. Atomizing system 1 was provided by Buchi (Switzerland), whereas the other two systems were provided by Spraying Systems Co. (United States).

The spray pattern is defined by the layout of the air cap orifices. Figure 1 depicts those corresponding to round and flat spray patterns.

2.1.2 Sprayed Molten Materials

Five grades of PEG with different molecular weights (MW) (1000, 1500, 2050, 4000, and 6000) were sprayed. Afterward, palmitic and stearic acids (PA and SA, respectively) were jointly sprayed (50 wt. %). All the materials were purchased from Sigma-Aldrich (France). Their physicochemical properties, at the different atomizing temperatures, are

TABLE 1: Characteristics of atomizing systems

		Dimensions (mm)		
Atomizing system	Spray pattern	d_L	d_a	A_a
1	Round	0.7	1.5	0.27
2	Round	0.7	1.62	0.79
3	Flat	0.5	1.7	0.86

Note. d_L = internal diameter of liquid orifice; d_a = internal diameter of air orifice (central orifice for atomizing system 3); A_a = cross-sectional area of the air. passage

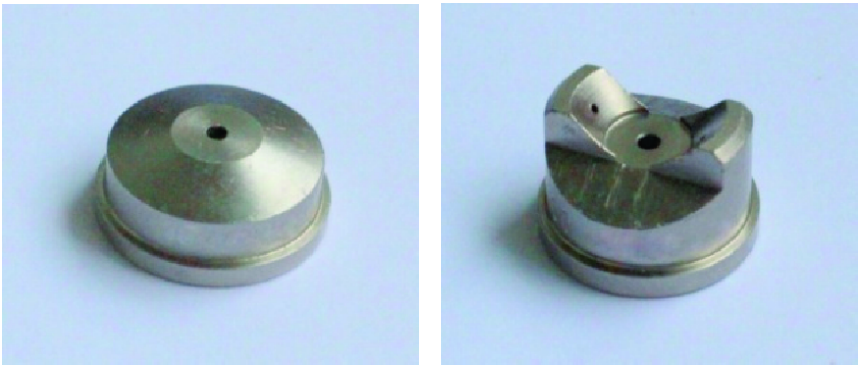

(a) (b)

FIG. 1: Air caps. (a) Round spray. (b) Flat spray.

presented in Tables 2 and 3. The melting points and viscosity values were determined according to Section 2.2. The data for surface tension and density were extracted/estimated from the literature (Dorinson et al., 1942; Hunten and Maass, 1929; Dee and Sauer, 1991; Chumpitaz et al., 1999; Cedeño González et al., 1999; Johansen and Schæfer, 2001).

2.2 Methods

2.2.1 Determination of Physicochemical Properties

2.2.1.1 Viscosity

For all the studied materials, the viscosity was measured with a rheometer Physica MCR 301 (Anton-Paar, Austria). A cone (49.974 mm, 0.998º, truncation: 101 μm) and a plate geometry was used over a shear rate range of 10^{-3}–10^{4} s^{-1}. All the materials showed non-Newtonian behavior, having reached, in all cases, a constant viscosity value for a shear rate as low as 5 s^{-1} (Fig. 2). Similar results were obtained for all the tested temperatures (data not shown).

For fluid flowing in a duct, a shear rate profile can be found inside liquid nozzles, for example, its maximum value is reached at the wall, while becoming zero along the

TABLE 2: Viscosity and melting point of molten materials

	Viscosity (mPa.s)				**Melting point (ºC)**	
Material	60ºC	70ºC	80ºC	90ºC	Range	Peak T
PEG						
1000	53	39	29	24	25–45	38
1500	—	65	51	41	45–60	52
2050	—	91	80	62	47–60	55
4000	—	—	262	204	49–66	61
6000	—	—	—	445	58–78	67
SA+PA 50% (w/w)	—	—	—	5.2	52–66	60

TABLE 3: Density and surface tension of molten materials

	Density (kg/m^3)				**Surface tension (mN/m)**			
Material	60ºC	70ºC	80ºC	90ºC	60ºC	70ºC	80ºC	90ºC
PEG								
1000	1096	1092	1085	1084	41.2	40.3	39.4	38.5
1500	1096	1092	1085	1084	—	40.7	39.8	38.9
2050	1096	1092	1085	1084	—	—	39.8	38.9
4000	1096	1092	1085	1084	—	—	39.6	38.8
6000	1096	1092	1085	1084	—	—	39.5	38.7
SA+PA 50% (w/w)	—	—	—	837.9	—	—	—	27.3

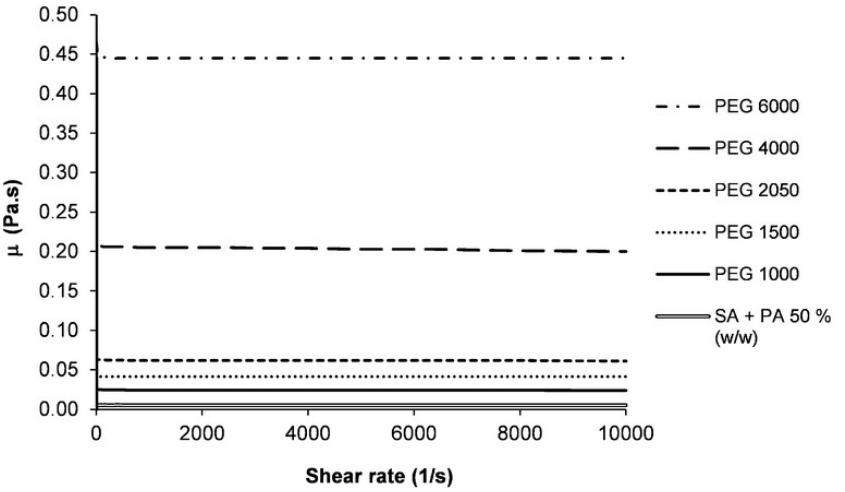

FIG. 2: Viscosity: Shear rate dependence for all materials tested at 90ºC.

center line of the flow. Nonetheless, at a two-fluid nozzle, a characteristic shear rate ($\dot{\gamma}$) can be estimated as a function of the average velocity (v_{av}) according to Eqs. (1) and (2) (Ghandi et al., 2012). The calculations for all the experimental conditions gave shear rate values of order 10^5–10^6 s^{-1}. Accordingly, and considering that constant viscosity values were reached for very low shear rates, all the materials were characterized by these representative viscosity values. Aliseda et al. (2008) followed the same criterion to determine the viscosity of non-Newtonian fluids sprayed with a two-fluid atomizer:

$$v_{av} = \frac{v_a \dot{m}_a + v_L \dot{m}_L}{\dot{m}_a + \dot{m}_L} \tag{1}$$

$$\dot{\gamma} = \frac{2(v_{av} - v_L)}{d_L} \tag{2}$$

where v_a/v_L is the air velocity to liquid velocity ratio, d_L is the inner nozzle diameter, and $\dot{m}_a/\dot{m}_L$ is the air mass flow rate to liquid mass flow rate ratio.

2.2.1.2 Melting Point

The melting point of the different materials was measured by differential scanning calorimetry (DSC) with a DSC131 evo (Setaram, France). The temperature program 10ºC–100ºC at 5ºC/min was used. All determinations were carried out under nitrogen atmosphere.

2.2.2 Atomizing Experiments

The raw material, after being melted in a thermostatic bath, was transported to the atomizing system by means of a peristaltic pump (Watson Marlow 323S, United Kingdom)

through heated hoses equipped with temperature controllers (RK Flex, France). The air pressure was registered upstream from the nozzle with a manometer (Wika, France), and the air flow rate was determined by means of a flowmeter FMA-A2417 (Omega, Canada). Experimental conditions for all the assays are detailed in Table 4.

The sprayed droplet size distributions were measured by laser diffraction with an Insitec Spray device (Malvern, United Kingdom), having a particle size range of 0.1–2500 μm. This device allows *in situ*, real-time particle size measurement for sprays and aerosols. As shown in Fig. 3, the nozzle was positioned perpendicularly to the laser beam. The distance between the nozzle exit and the laser beam was set to 10 cm. The software RT Sizer (Malvern, United Kingdom) was used to register the data and calculate the Sauter mean droplet diameter.

TABLE 4: Experimental conditions for the atomizing experiments

		T (ºC)					Air	
Atomizing system	Material	60	70	80	90	$\dot{m}_L$ (kg/h)	$P \times 10^{-2}$ (kPa)	$\dot{m}_a/\dot{m}_L$ (ALR)
1	PEG 1000	•	•		•	0.55	0.18–2.35	0.5–2.1
	PEG 1500		•		•	0.55		
	PEG 2050		•		•	0.55		
	PEG 4000			•	•	0.55		
	PEG 6000				•	0.55		
	SA+PA 50% (w/w)				•	0.55		
2	PEG 1000				•	0.55	0.02–1.7	0.6–6.3
3	PEG 1000				•	0.55	0.02–1.1	1.2–5.4

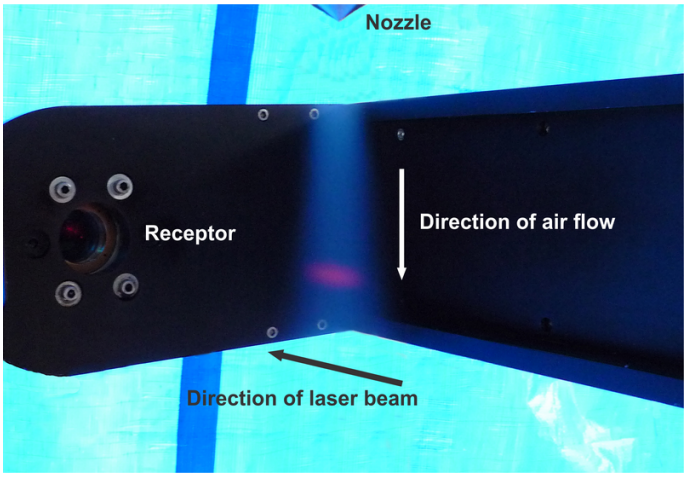

FIG. 3: Experimental setup.

2.2.3 Relative Span Factor (RSF) Calculation

The RSF was computed as follows:

$$\text{RSF} = \frac{d_{v,90} - d_{v,10}}{d_{v,50}} \tag{3}$$

where $d_{v,10}$, $d_{v,50}$, and $d_{v,90}$ correspond to the droplet sizes for which 10%, 50%, and 90% of the total volume distribution, respectively, is constituted by droplets of smaller sizes.

2.2.4 Fitting of Model Parameters

The fitting of the experimental data to the selected models was performed by means of a Microsoft Excel 2007 solver subroutine (Microsoft Corporation, United States). The sum of squares of the deviations between the experimental and predicted Sauter mean values was minimized.

3. MODELING: CORRELATIONS REPORTED IN THE OPEN LITERATURE

Probably the most well-known and cited work in the pneumatic atomization field is that performed by Nukiyama and Tanasawa (1939). By means of an internal mixing flat spray nozzle, different liquids (water, alcohol, heavy fuel oil, and gasoline) were atomized. The droplets were collected on glass plates covered with oil and further analyzed under a microscope to determine the drop sizes (Hede et al., 2008). Although the correlation was originally derived for an internal mixing nozzle, it has demonstrated an ability to correctly predict droplet sizes obtained with small external mixing nozzles under moderate air pressures and low liquid flow rates (Dewettinck, 1997).

Since the publication of that work, many researchers have addressed the study of sprays generated by pneumatic atomization of liquids. Most of them have been focused on low-viscosity fluid behavior. Indeed, the number of works dealing with the atomization of high-viscosity materials is considerably lower (Aliseda et al., 2008). Studies concerning the modeling of the mean droplet size generated by spraying molten materials with two-fluid nozzles are even scarcer. To the authors' knowledge, only two works have dealt with the collection and modeling of this type of experimental data. Kim and Marshall (1971) atomized molten wax and melts of wax–polyethylene mixtures (exhibiting a maximum viscosity of 49.2 mPa.s) by means of three concentric double air nozzle atomizers of their own design and a commercial one. Tsai and Viers (1990) atomized mixtures of PEG 8000 dissolved in PEG 600 with a modified commercial nozzle used in slurry combustion. Unlike the atomizers utilized in these two publications, the nozzles chosen to carry out the present study are commercially available. Besides, the ranges of viscosity, density, and surface tension covered in this work are wider. Therefore it is expected that the results reported here will find extended application.

Considering the limited availability of correlations to predict mean diameters of droplet distributions for the atomization of molten materials by using external mixing nozzles, five models derived for diverse types of liquids were selected from the open literature [see Eqs. (4)–(11)]. Table 5 summarizes the experimental conditions in which they were derived and the numerical values of their parameters. It is worth noting that the correlations presented by Tsai and Viers (1990) are not included because they predict the mass median diameter, instead of the Sauter mean diameter:

$$d_{32} = \frac{A}{v_{rel}} \left(\frac{\gamma_L}{\rho_L} \right)^{0.5} + B \left(\frac{\mu_L}{\sqrt{\gamma_L \rho_L}} \right)^{0.45} \left(\frac{1000\, Q_L}{Q_a} \right)^{C} \tag{4}$$

$$d_m = A \left[\left(\frac{1}{\mathrm{ALR}} \right) \left(\frac{\mu_a}{(\dot{m}_a / A_a)\, d_L} \right) \right]^{B} \tag{5}$$

$$\log d_m = \log d_{32} + 1.1513 \log^2 \sigma_g \tag{6}$$

$$\sigma_g = 1.77\, d_m^{0.14} \tag{7}$$

$$d_m = \left[\frac{A \gamma_L^{0.41} \mu_L^{0.32}}{\left(v_{rel}^2 \rho_L\right)^{0.57} A_a^{0.36} \rho_L^{0.16}} \right] + B \left[\left(\frac{\mu_L}{\gamma_L \rho_L} \right)^{0.17} \left(\frac{1}{v_{rel}^{0.54}} \right) \mathrm{ALR}^m \right] \tag{8}$$

$$d_{32} = 0.83\, d_m \tag{9}$$

where $m = -1.0$ if ALR < 3 and $m = -0.5$ if ALR > 3

$$d_{32} = A\, d_L \left[\frac{\left[(v_a^2 \rho_a d_L)/(\gamma_L) \right]}{\left(1 + (1/\mathrm{ALR})\right)^2} \right]^{B} \left(1 + C \frac{\mu_L}{\sqrt{\gamma_L \rho_L d_L}} \right) \tag{10}$$

$$d_{32} = \frac{A}{v_{rel}} \left(\frac{\gamma_L}{\rho_L} \right)^{0.5} + B \left(\frac{\mu_L}{\sqrt{\gamma_L \rho_L}} \right)^{0.45} \exp\left(\frac{-Q_a}{10^6 Q_L} \right) \tag{11}$$

where A, B, and C are model parameters; d_m is the mass median diameter (μm); σ_g is the geometric standard deviation (μm); v_{rel} is the relative velocity between air and liquid [m/s in Eqs. (4) and (11), ft/s in Eq. (8)]; γ_L is the liquid surface tension [dyn/cm in Eqs. (4), (8), and (11)]; ρ_L/ρ_a is the liquid density to air density ratio [g/cm^3 in Eqs. (4) and (11) and lb/ft^3 in Eq. (8)]; μ_L/μ_a is the liquid viscosity to air viscosity ratio [P in Eqs. (4), (5), and (11), cP in Eq. (8)]; Q_L/Q_a is the liquid volumetric flow rate to air volumetric flow rate ratio; $\dot{m}_a$ is air mass flow rate [lb/min in Eq. (5)]; A_a is the cross-sectional area of the air orifice [ft^2 in Eq. (5), in^2 in Eq. (8)]; d_L is the diameter of the liquid orifice [cm in Eq. (5)]; and ALR is the air to liquid mass flow rate ratio. Equation (10) is dimensionally correct.

Two important dimensionless numbers, which are widely used in droplet size characterization studies, appear in Eq. (10): the Weber number $\left[\mathrm{We}_a = (v_a^2 \rho_a d_L)/(\gamma_L)\right]$, given by the ratio of gas dynamic pressure to liquid capillary pressure (Walzel, 1993),

TABLE 5: Summary of the correlations extracted from the open literature

		Parameters			Atomization system				Liquid properties			Air properties			
Authors	Equation	A	B	C	Nozzle	Liquid diameter, d_L (mm)	Air diameter, d_a (mm)	Liquid	Viscosity (mPa.s)	Surface tension (mN/m)	Density (kg/m^3)	Pressure $\times 10^{-2}$ (kPa)	Velocity (m/s)	Mass ratio, $\dot{m}_a/\dot{m}_L$ (ALR)	Predicted d_{32} range (m)
Nukiyama and Tanasawa (1939)	(4)	585	597	1.5	Internal mixing, flat spray	0.2–1	1–5	Water, alcohol, heavy fuel oil, gasoline	1.0–5.0	19.0–73.0	700–1200	1	60–340	1–14	15–19
Gretzinger and Marshall (1961)	(5)–(7)	2600	0.4	–	External mixing, round spray	1.4–5.5	2.4–3.2	Aqueous solution of a black dye	1.0	50.0	1000	1.7–4.2	348	1–15	6.9–50
Kim and Marshall (1971)	(8)–(9)	249	1260	–	External mixing, round spray	3.1–6.9	1.4–5.6	Molten wax and melts of wax–polyethylene mixtures	8.7–49.2	29.6–31.2	782–834	0.76–2.0	75–393	0.06–40	10–160
Walzel (1993)	(10)	0.35	–0.4	0.25	External mixing, round spray	0.2–0.25	0.2–0.4	Water and aqueous glycerol solutions	1.0–100	64.0–72.0	950–1100	N/A	N/A	N/A	5–25
Kahen et al. (2005)	(11)	86.4	105.4	–	External mixing, round spray	0.10	0.16	Hexane, acetone, xylene, toluene, methanol, ethanol, water	0.33–1.20	18.4–72.8	660–1000	N/A	N/A	N/A	4.6–7.2

Note. N/A = not available.

and the Ohnesorge number $\left[\text{Oh} = (\mu_L)/(\sqrt{\gamma_L \rho_L d_L})\right]$, which accounts for the relative importance of stabilizing viscous forces to surface tension forces (Kashani, 2010).

4. RESULTS AND DISCUSSION

4.1 Sauter Mean Droplet Size (d_{32})

4.1.1 Effect of Temperature and Air to Liquid Mass Flow Rate Ratio (ALR)

Figure 4 presents the Sauter mean droplet size as a function of ALR at different temperatures for PEG 1000 atomized with the atomizing system 1 (see Table 1). It is worth mentioning that ALR is proportional to the atomizing air mass flow rate, because the liquid mass flow rate was kept constant for all the experiments.

As ALR decreases, d_{32} increases for the three tested temperatures, as should be expected for all the atomizing systems. At low ALR and 90ºC, the droplet size is smaller than those obtained for the other two temperatures. Analyzing the physicochemical properties of PEG 1000 (Tables 2 and 3), it can be observed that the surface tension and density do not change significantly when the temperature increases from 60ºC to 90ºC (–6.6% and –1.1%, respectively), whereas the viscosity does decrease substantially (55%). The lower the material viscosity is, the lower is its resistance to disaggregation and the higher is the number of smaller droplets generated. Conversely, at high ALR, the effect of an increase in the air kinetic energy is important enough to nullify the effect of the difference in viscosities.

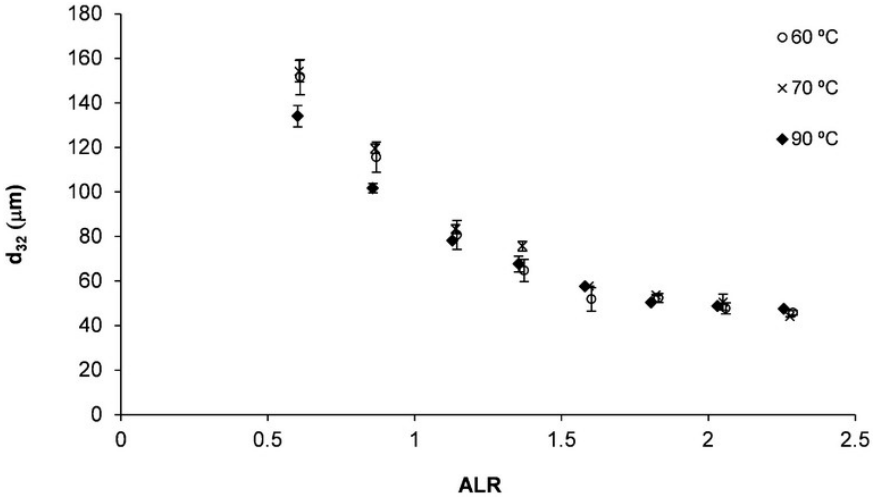

FIG. 4: Influence of atomized material temperature and air to liquid mass flow ratio (ALR) on mean droplet size for polyethylene glycol (PEG) 1000 and atomizing system 1 (Table 1).

4.1.2 Effect of Polyethylene Glycol Grade and ALR

Figure 5 depicts the influence of ALR on Sauter mean droplet size for all the PEG grades atomized with the atomizing system 1 (Table 1) at 90ºC.

It is evident that no significant differences were found in the mean droplet diameter for materials with MW ranging from 1000 to 2050 in comparison with PEG 4000 and 6000. The differences in viscosity between the first materials and these two latter highlight the important effect of this property on droplet size. For the materials with the highest viscosities (PEG 4000 and 6000), a lower sensitivity of the droplet diameter with ALR is observed, in accordance with results reported in the literature (Lefebvre, 1980).

4.2 Droplet Size Distribution

In Fig. 6, some examples of droplet size distributions (based on volume) are presented. Regarding the effect of temperature, as indicated earlier, the value of d_{32} obtained when PEG 1000 was atomized at 90ºC was smaller than the value corresponding to 70ºC. Consequently, a slight shift to lower droplet sizes can be observed at the higher temperature. The effect of ALR can be clearly described by comparing the droplet distributions at the lowest and highest ALR. In the first case, the low air flow rate cannot overcome the differences in the physicochemical properties of PEG 1000 and 2050 at 90ºC, both distributions being distinctly different. Conversely, for an ALR of 2.5, even though PEG 1000 and 4000 at 90ºC present significant differences in their physicochemical properties, the effect of the air flow rate compensates to a great extent these differences, leading to comparable d_{32} and droplet size distributions in accordance with this result.

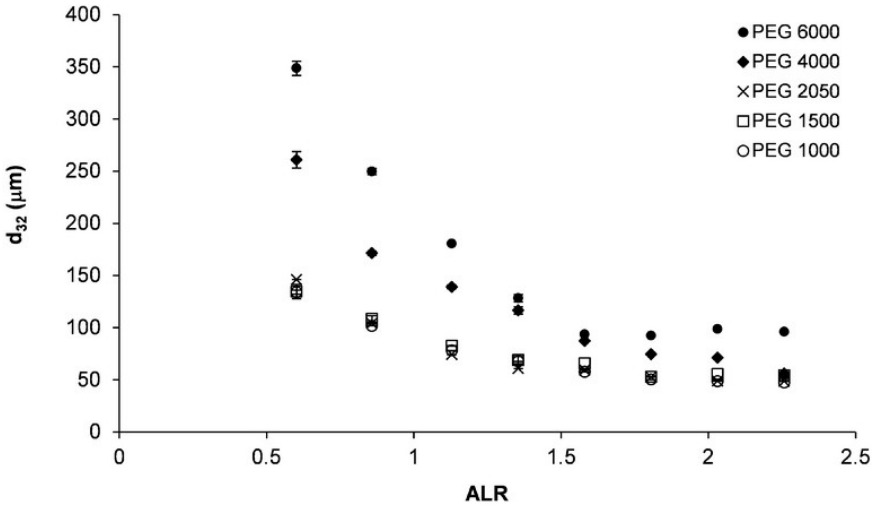

FIG. 5: Influence of PEG grade and ALR on mean droplet size for atomizing system 1 (Table 1) at 90ºC.

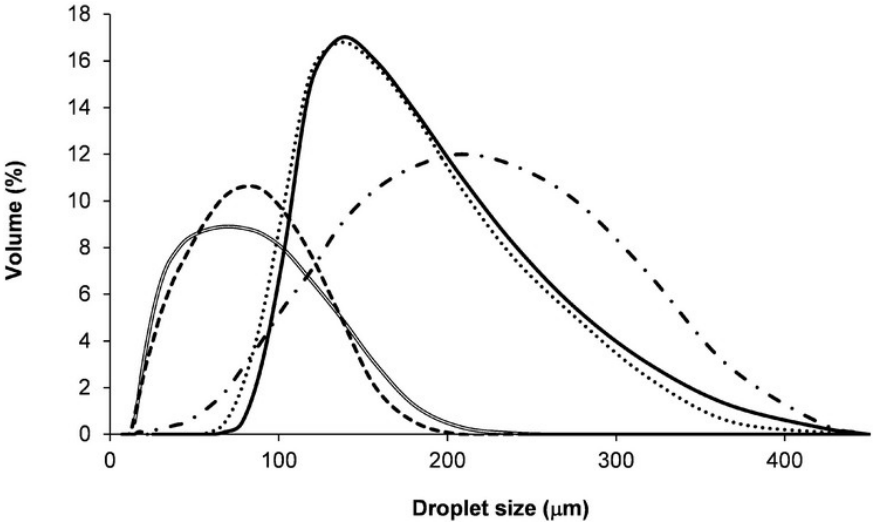

FIG. 6: Volume droplet size distributions: PEG 1000, 70ºC, ALR 0.6 (solid line); PEG 1000, 90ºC, ALR 0.6 (dotted line); PEG 2050, 90ºC, ALR 0.6 (dash-dotted line); PEG 1000, 90ºC, ALR 2.5 (dashed line); and PEG 4000, 90ºC, ALR 2.5 (double solid line).

4.3 RSF

Regarding the relative span factor, no correlation between experimental conditions and RSF was observed, having obtained mean RSF values of 1.09 ± 0.15, 1.19 ± 0.35, and 1.11 ± 0.25 for atomizing systems 1, 2, and 3, respectively. The closeness to unity of all three values indicates an excellent spray quality in terms of uniformity (Schick, 2008).

4.4 Prediction of Sauter Mean Droplet Size (d_{32})

First, and for all the experiments carried out with atomizing system 1, the Sauter mean droplet size was estimated by means of the correlations presented in Eqs. (4)–(11) with their original parameters (Table 5).

The Nukiyama–Tanasawa (NT) equation overestimated d_{32} for all the studied experimental conditions (data not shown). The greatest overestimations were at low ALR and high viscosities, the most severe case being approximately 11.6 times the experimental diameter. This result is not surprising; in fact, numerous authors have accounted for this behavior (Canals et al., 1990; Robles et al., 1992; Kahen et al., 2005; Kashani, 2010). The possible reasons for such discrepancies are various: the absence of nozzle dimensions in the equation; the subsonic conditions in which the NT experiments were performed by keeping the air density constant (Hede et al., 2008); the technique used to measure droplet size (collecting and observing them under a microscope, leading to a correlation that could be to some extent biased in favor of larger mean droplet moments; Kashani, 2010). Finally, the term (1000 Q_L/Q_a) took on values equal to or below unity

in the NT experiments, reducing the probability of an overestimation (Kashani, 2010). In the present experiments, the highest value for this term doubled that corresponding to the NT work.

With the aim of improving the prediction of the experimental data obtained with all grades of PEG at all the tested temperatures, the three parameters of the NT equation were fitted. When the fittings were carried out independently for each set of experimental conditions, it was observed that, for PEG with relatively low MW (1000–2050), parameters A and C did not show significant variations, unlike parameter B. To obtain a single equation capable of modeling this set of experimental data, parameter B was expressed as a function of the viscosity of the atomized material. As was stated earlier, this was the physicochemical property that showed the highest influence on the droplet mean diameter in the studied experimental domain. Regarding the fittings of the data corresponding to PEG with relatively high MW (4000 and 6000), the same procedure was performed, obtaining a viscosity-dependent parameter A and constant B and C. Table 6 presents the adjusted parameters and the corresponding coefficient of determination (R^2).

TABLE 6: Parameters adjusted for all the experiments carried out with atomizing system 1

	Parameter			
Correlation[a]	A	B	C	R^2
Nukiyama and Tanasawa (1939)[b]				
PEG 1000, 1500, 2050	13.958	$-416\ \mu^{-0.43}$	0.89	0.9148
PEG 4000, 6000	$2.82 \times 10^6\mu + 7.40 \times 10^6$	108	1.55	0.9364
Kahen et al. (2005)[b]				
PEG 1000, 1500, 2050	$846\mu + 3964$	$30.6\mu - 113$	—	0.9118
PEG 4000, 6000	$1658\mu + 4312$	$-11.3\mu - 90.3$	—	0.9458
Gretzinger and Marshall (1961)[b]	$4.89 \times 10^5\mu + 9.24 \times 10^5$	0.61	—	0.9264
Kim and Marshall (1971)[c]				
PEG 1000, 1500, 2050	$-2.35\mu + 641$	$-8.67\mu - 479$		0.9614
PEG 4000, 6000	339	$3.75\mu + 1110$	—	0.9628
Walzel (1993)[d]	$55.9\ \mu^{-0.66}$	–0.36	8191	0.9475

Note. See Table 4 for atomizing conditions.
[a] See Eqs. (4)–(11).
[b] Liquid viscosity expressed in P.
[c] Liquid viscosity expressed in mPa.s.
[d] Liquid viscosity expressed in Pa.s.

The predictions of the other correlations with the original parameters also gave unsatisfactory results owing to differences in materials' properties, atomizing systems, and operating conditions. Nonetheless, it was possible to fit their parameters, obtaining models capable of predicting the mean droplet size with R^2 higher than 0.91 (Table 6).

The correlations showing the best predictive capacity were those derived by Kim and Marshall (1971) and Walzel (1993), the latter having an additional advantage over the former, consisting in a single expression capable of predicting all the data throughout the studied experimental domain. Figure 7 presents, for all grades of PEG at all tested temperatures, the correlation between the experimental data and those predicted by means of the Walzel model. In particular, and as an example, the fittings of this model to the experimental data corresponding to all PEG grades at 90ºC are presented in Fig. 8.

4.5 Evaluation of the Models outside the Domain in Which They Were Derived

After the atomization of PEG with atomizing system 1, additional experiments with a mixture of stearic and palmitic acids (50 wt. %) were performed. The purpose of carrying out assays with a material having markedly different physicochemical properties than PEG (Tables 2 and 3) was to evaluate the predictive capacity of the models outside the range of experimental conditions in which they were derived. To this end, PEG 1000 was also atomized at 90ºC using atomizing systems 2 and 3 (Table 1), which had different dimensions and spray patterns than the one used to derived the correlations to be tested.

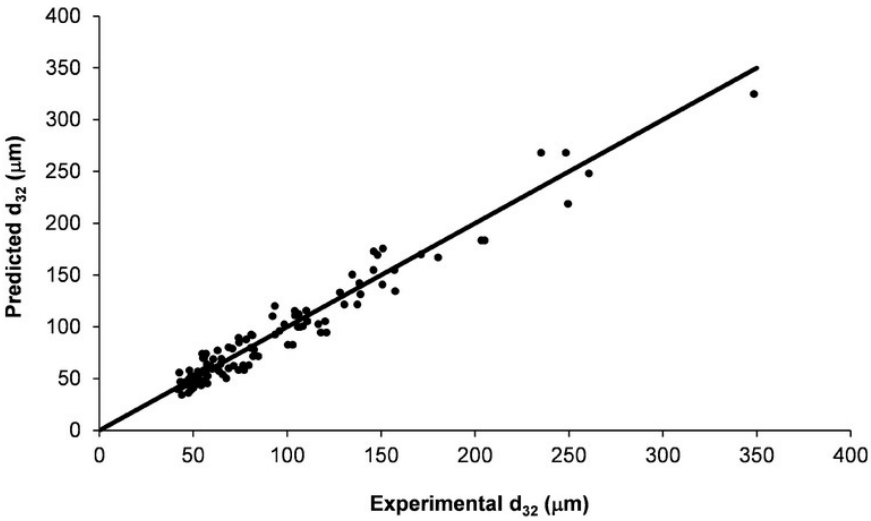

FIG. 7: Predicted versus experimental Sauter mean droplet diameter according to Walzel (1993) correlation with the parameters reported in Table 6 for all grades of PEG at all temperatures and atomizing system 1.

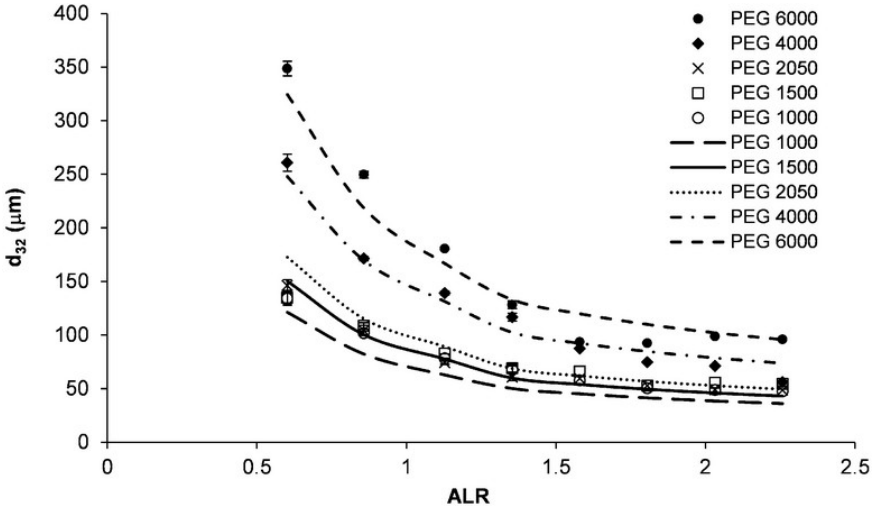

FIG. 8: Fittings for Walzel (1993) correlation with the parameters reported in Table 6 for PEG 1000, 1500, 2050, 4000, and 6000 at 90ºC with atomizing system 1.

The predictions of the models to this new data were not satisfactory for any of the experimental conditions. Therefore new parameter fittings were performed, obtaining models capable of predicting the Sauter mean droplet diameter for the fatty acid mixture or atomizing systems 2 and 3. The corresponding coefficients of determination show highly satisfactory fittings (Tables 7 and 8). It is evident that higher R^2 were obtained in comparison with those reported in Table 6 (i.e., for the data corresponding to different grades of PEG at different temperatures and atomizing system 1). Although the fittings were better for these new sets of data, it is important to note that the fittings with lower R^2 correspond to a much greater quantity of data, leading to more comprehensive correlations.

TABLE 7: Model parameters corresponding to the atomization of the stearic and palmitic acid mixture

	Parameter			
Correlation[a]	A	B	C	R^2
Nukiyama and Tanasawa (1939)	33.0	301	0.96	0.9883
Kahen et al. (2005)	2297	27.4	—	0.9887
Gretzinger and Marshall (1961)	1.04×10^5	0.46	—	0.9731
Kim and Marshall (1971)	1061	–3536	—	0.9776
Walzel (1993)	1327	–0.26	8272	0.9904

Note. See Table 4 for atomizing conditions.
[a]See Eqs. (4)–(11).

TABLE 8: Model parameters corresponding to spraying PEG 1000 with atomizing systems 2 and 3

		Parameter[a]			
Atomizing system	Correlation[b]	A	B	C	R^2
2	Nukiyama and Tanasawa (1939)	-8.64×10^5	2.09×10^5	1.00	0.8059
	Kahen et al. (2005)	1401	121	—	0.9647
	Gretzinger and Marshall (1961)	4.90×10^4	0.38	—	0.9962
	Kim and Marshall (1971)	924	–8851	—	0.9905
	Walzel (1993)	356	–0.22	8099	0.9878
3	Nukiyama-Tanasawa (1939)	2.67×10^5	-4.97×10^4	1.00	0.9767
	Kahen et al. (2005)	2409	–42.3	—	0.9589
	Gretzinger and Marshall (1961)	2.33×10^6	0.63	—	0.9722
	Kim and Marshall (1971)	358	1024	—	0.9648
	Walzel (1993)	1466	–0.45	7858	0.9613

Note. See Table 4 for atomizing conditions.

5. CONCLUSIONS

Several atomizing experiments of molten materials (PEG and a mixture of stearic and palmitic acid) at different temperatures and using different two-fluid external mixing nozzles were performed with the aim of characterizing the sprays by measuring the mean droplet diameter (d_{32}). The extent to which an increase in the material viscosity, as well as in ALR, causes a decrease in d_{32} was studied for different grades of PEG atomized at different temperatures with a given nozzle. Furthermore, the capacity of different d_{32} correlations reported in the open literature to predict the obtained experimental data was also evaluated. Once their inefficiency was demonstrated, certain parameters of the models were fitted, obtaining models capable of satisfactorily predicting the mean droplet diameter for the atomization of different grades of PEG, at different temperatures and ALR, with the same atomizing system. However, as these models showed poor performance in predicting the experimental data corresponding to the spraying of fatty acids with the same atomizing system and the spraying of PEG with different nozzles, the parameters were fitted again to obtain models that were valid for the new experimental conditions.

In summary, the application of the selected models from the literature to the atomization of molten materials does not lead to a correct prediction of the Sauter mean droplet diameter in a wide range of experimental conditions (i.e., nature of the molten material, operating conditions, and atomizing system). In this sense, considering that the viscosity of the atomized material was the physicochemical property with the highest variability

over the experimental domain studied, and with the aim of extending the range of validity of the models, it was proposed to express certain model parameters as a function of the liquid viscosity. For the atomization of different PEG grades with a given atomizing system at different temperatures and ALR, the strategy proved to be highly satisfactory in predicting the Sauter mean droplet size.

ACKNOWLEDGMENTS

This work received financial support from the Conseil Régional de Picardie (France), the Consejo Nacional de Investigaciones Científicas y Técnicas (CONICET), the Agencia Nacional de Promoción Científica y Tecnológica (ANPCyT), and the Universidad Nacional del Sur (UNS) (Argentina).

REFERENCES

Aliseda, A., Hopfinger, E. J., Las Heras, J. C., Kremer, D. M., Berchielli, A., and Connolly, E. K., Atomization of viscous and non-Newtonian liquids by a coaxial, high-speed gas jet: Experiments and droplet size modeling, *Int. J. Multiphase Flow*, vol. **34**, pp. 161–175, 2008.

Borini, G. B., Andrade, T. C., and Freitas, L. A. P., Hot melt granulation of coarse pharmaceutical powders in a spouted bed, *Powder Technol.*, vol. **189**, pp. 520–527, 2009.

Bose, S. and Bogner, R., Solventless pharmaceutical coating processes: A review, *Pharma. Dev. Technol.*, vol. **12**, no. 2, pp. 115–131, 2007.

Canals, A., Hernandis, V., and Browner, R. F., Experimental evaluation of the Nukiyama–Tanasawa equation for pneumatic nebulisers used in plasma atomic emission spectrometry, *J. Anal. Atomic Spectrometry*, vol. **5**, pp. 61–66, 1990.

Cedeño González, F. O., Prieto González, M., Bada Gancedo, J. C., and Suárez, R. A., Estudio de la densidad y de la viscosidad de algunos ácidos grasos puros, *Grasas y Aceites*, vol. **50**, pp. 359–368, 1999.

Chumpitaz, L., Coutinho, L. F., and Meirelles, A. J. A., Surface tension of fatty acids and triglycerides, *J. Am. Oil Chemists' Soc.*, vol. **76**, no. 3, pp. 379–382, 1999.

Dee, G. and Sauer, B., The molecular weight and temperature dependence of polymer surface tension: Comparison of experiment with interface gradient theory, *J. Colloid Interface Sci.*, vol. **152**, no. 1, pp. 85–103, 1991.

Dewettinck, K., Fluidized bed coating in food technology: Process and product quality, PhD thesis, University of Ghent, 1997.

Dorinson, A., McCorkle, M. R., and Ralston, A. W., Refractive indices and densities of normal saturated fatty acids in the liquid state, *J. Am. Oil Chemists' Soc.*, vol. **64**, no. 12, pp. 2739–2741, 1942.

Ejim, C. E., Rahman, M. A., Amirfazli, A., and Fleck, B. A., Effects of liquid viscosity and surface tension on atomization in two-phase, gas/liquid fluid coker nozzles, *Fuel*, vol. **89**, pp. 1872–1882, 2010.

Genbao, L., Jianming, C., Minglong, L., Yuhua, Q., and Zhaoyang, C., Experimental study on the

size distribution characteristics of spray droplets of DME/diesel blended fuels, *Fuel Process. Technol.*, vol. **104**, pp. 352–355, 2012.

Ghandi, A., Powell, I. B., Howes, T., Chen, X. D., and Adhikari, B., Effect of shear rate and oxygen stresses on the survival of *Lactococcus lactis* during the atomization and drying stages of spray drying: A laboratory and pilotscale study, *J. Food Eng.*, vol. **113**, pp. 194–200, 2012.

Gretzinger, J. and Marshall, W. R., Jr., Characteristics of pneumatic atomisation, *AIChE J.*, vol. **7**, no. 2, pp. 312–318, 1961.

Hede, P. D., Bach, P., and Jensen, A. D., Two-fluid spray atomization and pneumatic nozzles for fluid bed coating/agglomeration purposes: A review, *Chem. Eng. Sci.*, vol. **63**, pp. 3821–3842, 2008.

Hunten, K. W. and Maass, O., Investigation of surface tension constants in an homologous series from the point of view of surface orientation, *J. Am. Oil Chemists' Soc.*, vol. **51**, pp. 153–165, 1929.

Jiménez, T., Agglomération de particules par voie humide en lit fluidisé, PhD thesis, École Nationale Supérieure des Industries Agricoles et Alimentaires, 2007.

Johansen, A. and Schæfer, T., Effects of interactions between powder particle size and binder viscosity on agglomerate growth mechanisms in a high shear mixer, *Eur. J. Pharma. Sci.*, vol. **12**, pp. 297–309, 2001.

Kahen, K., Acon, B. W., and Montaser, A., Modified Nukiyama–Tanasawa and Rizk–Lefebvre models to predict droplet size for microconcentric nebulizers with aqueous and organic solvents, *J. Anal. Atomic Spectrom.*, vol. **20**, pp. 631–637, 2005.

Kashani, A., Aerosol characterization and analytical modeling of concentric pneumatic and flow focusing nebulizers for sample introduction, PhD thesis, Mechanical and Industrial Engineering Department, University of Toronto, 2010.

Kim, K. Y. and Marshall, W. R., Drop-size distributions from pneumatic atomisers, *AIChE J.*, vol. **17**, no. 3, pp. 575–584, 1971.

Kulah, G. and Kaya, O., Investigation and scale-up of hot-melt coating of pharmaceuticals in fluidized beds, *Powder Technol.*, vol. **208**, pp. 175–184, 2011.

Lefebvre, A. H., Airblast atomization, *Progr. Energy Combust. Sci.*, vol. **6**, pp. 233–261, 1980.

Lefebvre, A. H., Properties of sprays, *Particle Particle Syst. Characterization*, vol. **6**, pp. 176–186, 1989.

Mandato, S., Rondet, E., Delaplace, G., Barkouti, A., Galet, L., Accart, P., Ruiz, T., and Cuq, B., Liquids' atomization with two different nozzles: Modeling of the effects of some processing and formulation conditions by dimensional analysis, *Powder Technol.*, vol. **224**, pp. 323–330, 2012.

Nukiyama, S. and Tanasawa, Y., An experiment on atomisation of liquid: The effect of the properties of liquid on the size of drops, *Trans. ASME JSME J.*, vol. **18**, no. 5, pp. 68–75, 1939.

Nuyttens, D., Baetens, K., De Schampheleire, M., and Sonck, B., Effect of nozzle type, size and pressure on spray droplet characteristics, *Biosyst. Eng.*, vol. **97**, pp. 333–345, 2007.

Rizkalla, A. A. and Lefebvre, A. H., The influence of air and liquid properties on airblast atomisation, *J. Fluids Eng.*, vol. **97**, no. 3, pp. 316–320, 1975.

Robles, C., Mora, J., and Canals, A., Experimental evaluation of the Nukiyama–Tanasawa equa-

tion for pneumatically generated aerosols used in flame atomic spectrometry, *J. Appl. Spectrosc.*, vol. **4**, pp. 669–676, 1992.

Saleh, K. and Guigon, P., Coating and encapsulation processes in powder technology, in *Handbook of Powder Technology*, eds. Salman, A. D., Hounslow, M. J., and Seville, J. P. K., Amsterdam: Elsevier, pp. 323–375, 2007a.

Saleh, K. and Guigon, P., Influence of wetting parameters on particle growth in fluidized-bed coating and agglomeration processes, *Particle Particle Syst. Characterization*, vol. **24**, no. 2, pp. 136–143, 2007b.

Schick, R., Spray Technology Reference Guide: Understanding Drop Size, retrieved April 9th, http://www.spray.com/literature_pdfs/B459C_Understanding_Drop_Size.pdf, 2008.

Semião, V., Andrade, P., and Carvalho, M. G., Spray characterization: Numerical prediction of Sauter mean diameter and droplet size distribution, *Fuel*, vol. **75**, pp. 1707–1714, 1996.

Tsai, S. C. and Viers, B., Airblast atomization of viscous liquids, *Fuel*, vol. **69**, pp. 1412–1419, 1990.

Walzel, P., Liquid atomisation, *Int. Chem. Eng.*, vol. **33**, no. 1, pp. 46–60, 1993.

Walzel, P., Spraying and atomizing of liquids, in *Ullmann's Encyclopedia of Industrial Chemistry*, Weinheim: John Wiley, 2012.